

# SURFACE MORPHOLOGY OF $\text{Fe}_{79}\text{Mo}_8\text{Cu}_1\text{B}_{12}$ RIBBONS CHARACTERISED BY ATOMIC FORCE MICROSCOPY

Milan Pavúk<sup>1</sup>, Marcel Miglierini<sup>1,2</sup>, Milan Vůjtek<sup>2</sup>, Radek Zbořil<sup>2</sup>, Miroslav Mašláň<sup>2</sup> and Peter Švec<sup>3</sup>

<sup>1</sup>Department of Nuclear Physics and Technology, Faculty of Electrical Engineering and Information Technology, Slovak University of Technology, Ilkovičova 3, 812 19 Bratislava, Slovak Republic

<sup>2</sup>Nanomaterials Research Centre, Svobody 26, 771 46 Olomouc, Czech Republic

<sup>3</sup>Institute of Physics, Slovak Academy of Sciences, Dúbravská cesta 9, 845 11 Bratislava, Slovak Republic

Received: March 29, 2008

**Abstract.** In the present work, we have investigated progress of crystallization in the  $\text{Fe}_{79}\text{Mo}_8\text{Cu}_1\text{B}_{12}$  alloy as a function of annealing temperature. It was found that the sample is not completely amorphous in the as-quenched state. The results from atomic force microscopy accompanied by X-ray diffraction show that the crystallization at the wheel-side (i.e. the side which has been in contact with the rotating wheel during production) of the ribbon is more developed than on the opposite side. Changes in surface morphology are discussed against increasing temperature of annealing.

## 1. INTRODUCTION

Nanocrystalline Fe-based alloys represent a class of excellent magnetically soft materials. Their unique structural and magnetic properties have been reported in several papers [1,2]. Such magnetic properties are very favourable for technical applications in power transformers, magnetic heads, pulsed transformers, sensors and magnetic shielding. The nanocrystalline structure is obtained during the first crystallization stage, where nanometer-sized grains remain isolated from one another in an amorphous ferromagnetic matrix [3]. Structural changes, induced by annealing, modify the macroscopic magnetic behaviour of the constituent material. According to [4], some reports suggested that the formation of crystallites occurs more easily at the surface rather than in the bulk.

In this paper, we present our study on structural changes taking place at the surface and bulk regions during the crystallization process of  $\text{Fe}_{79}\text{Mo}_8\text{Cu}_1\text{B}_{12}$  alloy. We have devoted our interest to the study of this alloy which features a

NANOPERM-like structure similar to that of  $\text{Fe}_{76}\text{Mo}_8\text{Cu}_1\text{B}_{15}$ . The latter has proved to be a very good model system for investigation of crystallization phenomena as well as behaviour of hyperfine interactions [5]. Our work was motivated by better understanding of Mo-containing nanocrystalline systems which seem to be appropriate candidates especially for case studies of hyperfine interactions.

## 2. EXPERIMENTAL DETAILS

The as-quenched ribbon 10 mm wide and 20-22  $\mu\text{m}$  thick of nominal composition  $\text{Fe}_{79}\text{Mo}_8\text{Cu}_1\text{B}_{12}$  was prepared by rapid quenching on a copper wheel rotating with the velocity of  $35 \text{ ms}^{-1}$ . Chemical composition of the alloy was checked by emission spectrometry with inductively coupled plasma. Approximately 2 cm long pieces of the ribbon were annealed in vacuum at temperature range from 330 to 650  $^{\circ}\text{C}$  for 1 hour holding time to prepare samples with different contents of crystallites. Individual treatment temperatures were chosen according to differential scanning calorimetry (DSC) curve mea-

Corresponding author: Milan Pavuk, milan.pavuk@stuba.sk

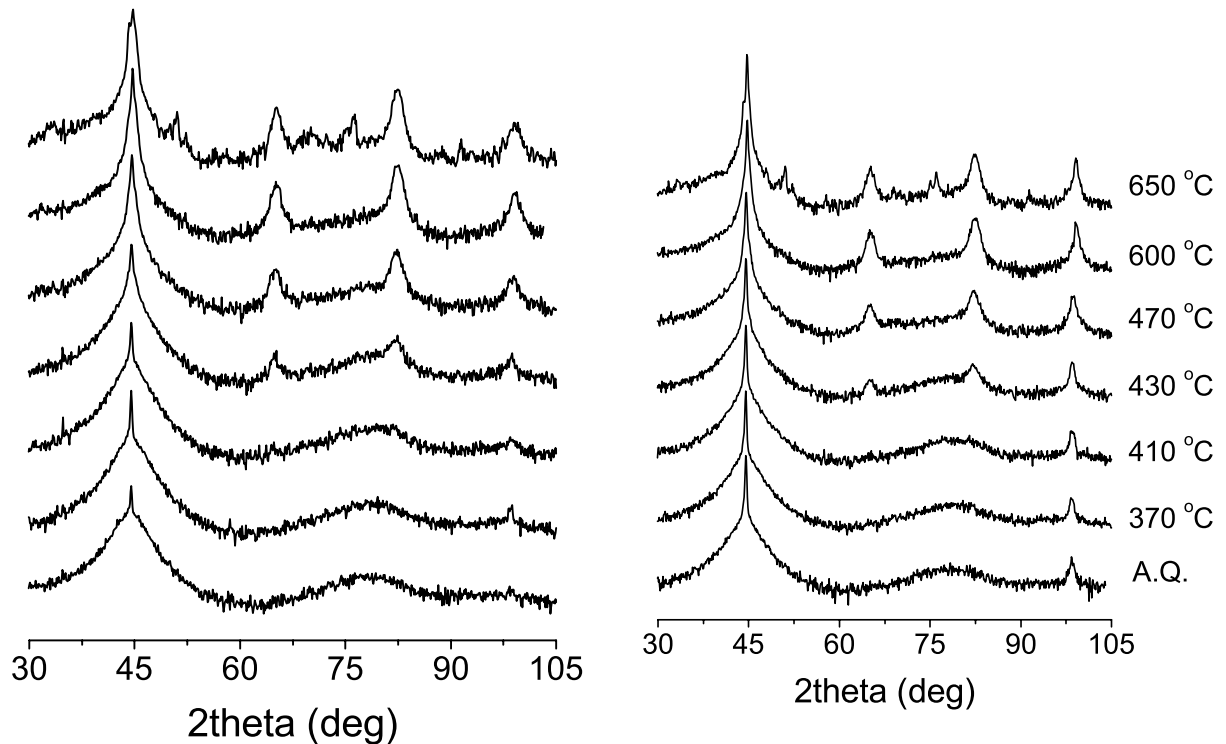


**Fig. 1.** X-ray diffraction patterns of  $Fe_{79}Mo_8Cu_1B_{12}$  alloy obtained from air (left) and wheel-side (right) of the ribbon for the as-quenched alloy (A.Q.) and annealed state. The vertical axes are in logarithmic scale.

sured on our sample in Ar atmosphere using PerkinElmer DSC 7 with the heating rate of 10 K/min [6]. The microstructure of as-quenched and nanocrystalline samples was analyzed by X-ray diffraction (XRD) with  $Cu-K_{\alpha}$  radiation and atomic force microscopy (AFM) operating in the non-contact mode. For the acquisition of topographic images, the AFM Explorer microscope (ThermoMicroscopes, USA) was used. The measurements were carried out under ambient conditions using silicon cantilevers of 1650-00 type from Veeco instruments. The tip radius is specified to be smaller than 10 nm. Prior to imaging, the probe tip was checked carefully for contamination by analysis of the calibration grid. When contamination was present, the probe was removed from the instrument and replaced. The measured data were processed with SPMLab software.

Throughout this paper we will use the following convention as far as the ribbon surfaces are concerned. The side of the ribbon, which was in direct contact with the quenching wheel, will be referred to as the wheel-side. The opposite side of the ribbon, i.e. which was exposed to the surrounding

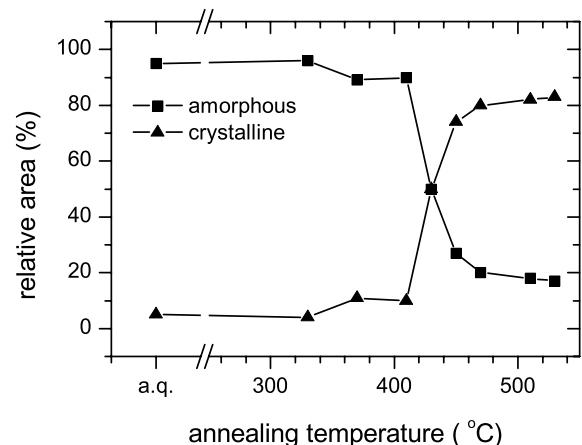


**Fig. 2.** Relative volume fraction of amorphous (squares) and crystalline (triangles) phase plotted against temperature of annealing as derived from XRD measurements performed upon the air-side of the ribbons. The solid curve is a guide to the eye.

atmosphere – visually shiny, will be denoted as the air-side.

### 3. RESULTS AND DISCUSSION

The crystallization behaviour of the as-quenched  $Fe_{79}Mo_8Cu_1B_{12}$  alloy was investigated using a DSC

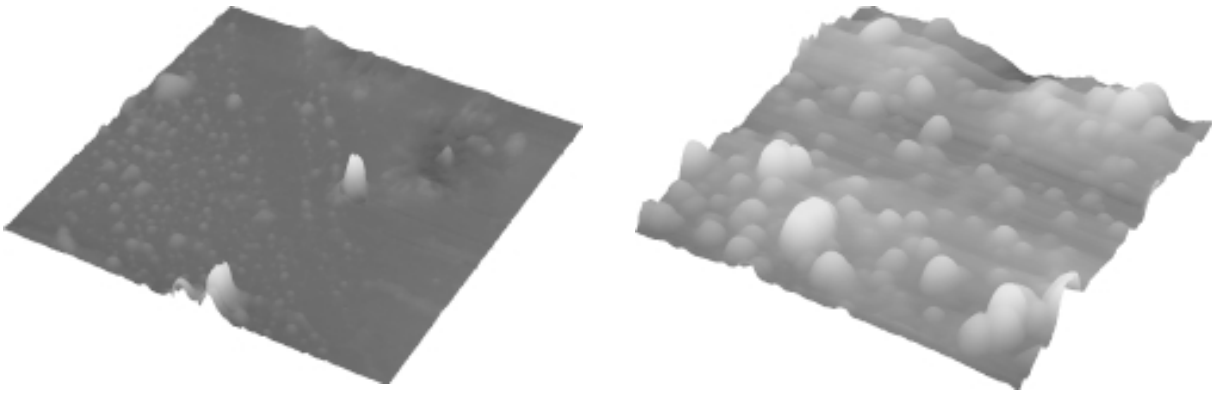


**Fig. 3.** AFM surface images of  $1 \times 1 \mu\text{m}^2$  area on the air (left) and wheel-side (right) of as-prepared  $\text{Fe}_{79}\text{Mo}_8\text{Cu}_1\text{B}_{12}$  specimen. The maximum of the vertical scale is 35 and 46 nm for the air and wheel-side image, respectively.

linear heating curve. The record is characterized by a massive exothermic peak which corresponds to the main crystallization step. The onset temperature of crystallization is observed at  $T_{x1} \cong 445 \text{ }^\circ\text{C}$  [6]. Taking the results of DSC measurements into account, we have selected the temperatures of annealing.

The XRD patterns of as-quenched sample presented in Fig. 1 were obtained from both air- and wheel-sides of the ribbon. They exhibited a broad peak at around  $2\theta = 44.5^\circ$ , often known as diffuse halo, which reflects the amorphous nature of the as-prepared specimens. Nevertheless, a narrow line superimposed on a broad peak indicates a presence of a nanocrystalline phase dispersed within the amorphous matrix. When comparing the principal X-ray reflections taken from both sides of the as-quenched  $\text{Fe}_{79}\text{Mo}_8\text{Cu}_1\text{B}_{12}$  ribbon, the crystallization at the wheel-side is clearly more developed. While the origin of the higher number density of nanocrystals on one particular side is still not clear, the opposite surfaces of a metallic glass ribbon are inherently non-uniform due to asymmetrical nature of the single-roll quenching techniques [7]. Structural inhomogeneities and/or high-stress regions [8] introduced during rapid solidification, considering the cooling rate distribution across the cross-section of a ribbon, can be responsible for the different degree of crystallization detected on both sides of the sample. The crystalline and amorphous contributions in Fig. 2 have been resolved by fitting the main diffraction peak

by means of different Pearson V II functions. For the as-prepared sample, the analysis of the results revealed that contribution of crystalline phase at the air-side is around 5 vol.% in the measured depth by the X-rays. For samples annealed at moderate temperatures, no notable changes in volume ratio of constituent phases were observed. The onset temperature of primary crystallization as derived from XRD is identified for 1 hour annealing at  $430 \text{ }^\circ\text{C}$  by appearance of peaks positioned over broad (amorphous) reflections; as expected, the sole product of the primary crystallization is bcc-Fe phase. With increasing temperature, the intensities of the bcc-Fe reflections are growing which corresponds to an increase of the volume fraction of this phase. Finally, after annealing at  $650 \text{ }^\circ\text{C}$ , presence of additional crystalline phases such as  $\text{Fe}_{0.875}\text{Mo}_{0.125}$ ,  $\text{Mo}_2\text{FeB}_2$ ,  $\text{Fe}_{23}\text{B}_6$  and  $\text{Fe}_3\text{B}$ , can be observed, to be formed fully at still higher temperatures.

More detailed information about the surface structure and the direct image of the crystallites on sample surface can also be obtained with AFM. The air-side of the as-quenched  $\text{Fe}_{79}\text{Mo}_8\text{Cu}_1\text{B}_{12}$  ribbon presents a smooth surface texture with brighter regions extending out of the ribbon plane (Fig. 3, left) which we will call protrusions. Few of them are quite well developed. The wheel-side of the scanned sample exhibited a wavy surface with notably more protrusions on it (Fig. 3, right). Undulation of the surface at this side of the ribbon could be explained as production mark due to physical

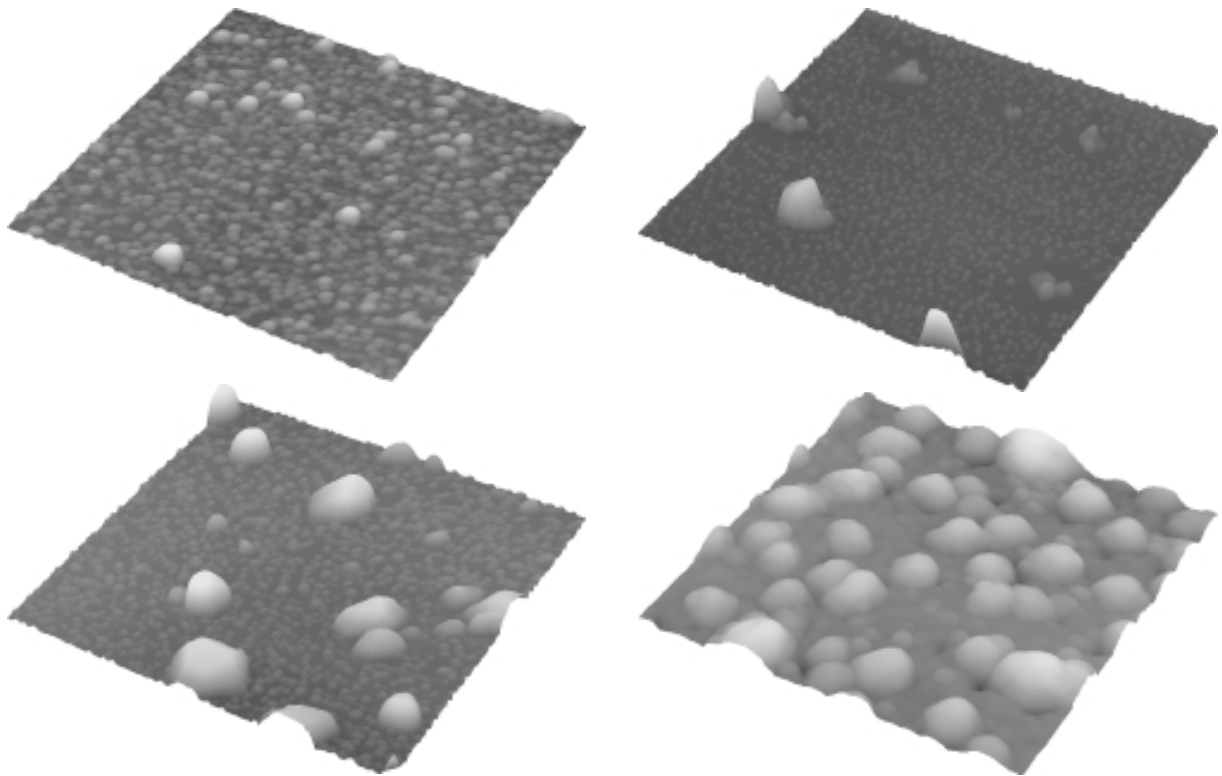


**Fig. 4.** Top: 3D AFM images from area  $2 \times 2 \mu\text{m}^2$  obtained from the air-side of  $\text{Fe}_{79}\text{Mo}_8\text{Cu}_1\text{B}_{12}$  specimens annealed at 370 (left) and 410 °C (right) for 1 hour. The maximum of the vertical scale is 46 and 177 nm for the left and right image, respectively. Bottom: Surface morphological developments in the alloys annealed at 470 (left) and 650 °C (right). The maximum of the vertical scale is 127 nm in both images.

contact with the quenching wheel. This is the reason why we have concentrated on the inspection of the air-side of the specimens. Two types of protrusions different in size are visible on the wheel surface - large number of small sized dense protrusions with an average height of 1 nm and notably smaller number of higher columnar structures mostly 10-20 nm in height. The latter could confirm the evidence of crystallinity observed in XRD patterns even at temperatures below 400 °C (Fig. 1). Positioning of the scanning tip to different location unveiled even larger protrusions and no evidence of smaller (1 nm) ones. AFM pictures illustrated in Fig. 4 show the air side morphology of selected  $\text{Fe}_{79}\text{Mo}_8\text{Cu}_1\text{B}_{12}$  samples in the annealed state. It is clearly seen from this figure that the density of bright spots is directly related to the temperature of annealing, i.e. to the relative volume fraction of nanocrystallites formed in the alloy. The surface morphology observed at 410 °C is especially interesting. It shows very few large objects of

non-uniform shape that are surrounded by small sized protrusions with rather uniform height (10 nm) and closely packed structure. Finally, in the sample annealed at 650 °C, the particle size has increased drastically. It is noteworthy that at this temperature of annealing a presence of additional (boron-containing) crystalline phases is evidenced by XRD. Thus, we suppose that the observed features are agglomerates of crystalline grains presumably composed of different phases which are, moreover, overlapping one another.

#### 4. CONCLUSIONS

The studied  $\text{Fe}_{79}\text{Mo}_8\text{Cu}_1\text{B}_{12}$  NANOPERM-type alloy is not fully amorphous (non-crystalline) even in the as-quenched state. Presence of small amount of crystalline bcc-Fe phase was confirmed at the surface by AFM. They are more abundant on the wheel-side of the ribbon as compared with the air-side.

The temperature of the onset of bulk crystallization was determined from DSC to be of 445 °C [6]. XRD shows appearance of thermally induced crystallization at 430 °C. This slight apparent deviation can be explained by different temperature profiles applied during DSC scan and preparation of nanocrystalline alloy by annealing. While during the first (dynamic) treatment the system is exposed to varying temperature with time the latter conditions are isothermal and enable enough time for structural transformations which, consequently, appear at lower temperature.

## ACKNOWLEDGEMENTS

The authors are grateful to E. Illeková (Bratislava) for assistance with DCS measurements. This work was supported by the grants MSM6198959218, V EGA 1/4011/07, APV T-51-052702, APV T-20-008404, and CEX Nanosmart.

## References

- [1] G. Herzer // *Phys. Scr.* **49** (1993) 307.
- [2] M. E. McHenry and D. E. Laughlin // *Acta Mater.* **48** (2000) 223.
- [3] I. Bibicu, J.S. Garitaonandia, F. Plazaola and E. Apiñaniz // *J. Non-Cryst. Solids* **287** (2001) 277.
- [4] A-T. Le, Ch-O. Kim, N. Chau, N.D. Cuong, N.D. Tho, N.Q. Hoa and H. Lee // *J. Magn. Magn. Mater.* **307** (2006) 178.
- [5] M. Miglierini, J. Degmová, T. Kaňuch, P. Švec, E. Illeková and D. Janičkovič, In: *Properties and Applications of Nanocrystalline Alloys from Amorphous Precursors*, ed. by B. Idzikowski *et al.* (Kluwer Acad. Publ., 2005), p. 421.
- [6] E. Illeková, D. Janičkovič, M. Miglierini, I. Škorvánek and P. Švec // *J. Magn. Magn. Mater.* **304** (2006) e636.
- [7] Y. Birol // *Mater. Sci. Eng. A* **249** (1998) 79.
- [8] T. Egami, K. Maeda and V. Vitek // *Phil. Mag. A* **41** (1980) 883.